Role of High-Resolution Dynamic Contrast-Enhanced MRI with Golden-Angle Radial Sparse Parallel Reconstruction to Identify the Normal Pituitary Gland in Patients with Macroadenomas

R. Sen, C. Sen, J. Pack, K.T. Block, J.G. Golfinos, V. Prabhu, F. Boada, O. Gonen, D. Kondziolka, and G. Fatterpekar

ABSTRACT

BACKGROUND AND PURPOSE: Preoperative localization of the pituitary gland with imaging in patients with macroadenomas has been inadequately explored. The pituitary gland enhancing more avidly than a macroadenoma has been described in the literature. Taking advantage of this differential enhancement pattern, our aim was to evaluate the role of high-resolution dynamic MR imaging with golden-angle radial sparse parallel reconstruction in localizing the pituitary gland in patients undergoing trans-sphenoidal resection of a macroadenoma.

MATERIALS AND METHODS: A retrospective study was performed in 17 patients who underwent trans-sphenoidal surgery for pituitary macroadenoma. Radial volumetric interpolated brain examination sequences with golden-angle radial sparse parallel technique were obtained. Using an ROI-based method to obtain signal-time curves and permeability measures, 3 separate readers identified the normal pituitary gland distinct from the macroadenoma. The readers' localizations were then compared with the intraoperative location of the gland. Statistical analyses were performed to assess the interobserver agreement and correlation with operative findings.

RESULTS: The normal pituitary gland was found to have steeper enhancement-time curves as well as higher peak enhancement values compared with the macroadenoma ($P < .001$). Interobserver agreement was almost perfect in all 3 planes ($\kappa = 0.89$). In the 14 cases in which the gland was clearly identified intraoperatively, the correlation between the readers' localization and the true location derived from surgery was also nearly perfect ($\kappa = 0.95$).

CONCLUSIONS: This study confirms our ability to consistently and accurately identify the normal pituitary gland in patients with macroadenomas with the golden-angle radial sparse parallel technique with quantitative permeability measurements and enhancement-time curves.

ABBREVIATIONS: ETC = enhancement-time curve; GRASP = golden-angle radial sparse parallel

Hormonal deficiency is a major complication of trans-sphenoidal surgery for pituitary adenomas.[1-3] While the trans-sphenoidal approach offers optimal access to the sellar and suprasellar regions,[4-8] approximately 5% of patients experience new hypopituitarism due to excision of or damage to the normal pituitary gland.[9] In the case of large macroadenomas, this complication is often due to poor visualization of the gland, which is markedly attenuated and displaced by the tumor.

Given the importance of preserving the gland, localization with preoperative imaging will be of use to surgeons. Although

dynamic MR imaging is the criterion standard for radiographic evaluation of pituitary adenomas,[10] its role in preoperative localization of the pituitary gland in patients with macroadenomas has not been adequately explored.

Golden-angle radial sparse parallel (GRASP) MR imaging is a new volumetric dynamic technique based on a 3D gradient-echo sequence with radial "stack-of-stars" k-space sampling[11,12] and golden-angle ordering.[13,14] The GRASP technique acquires all dynamic information in a single, continuous scan after contrast is introduced. Images are reconstructed iteratively by combining signals from all coils and using compressed sensing,[12,15] which enables reconstructing images from largely undersampled data. These unique characteristics allow GRASP to obtain images with both high spatial and temporal resolution. While GRASP-acquired permeability measurements, including signal-enhancement patterns of the normal pituitary gland, have been demonstrated,[16] its role in the evaluation of macroadenomas has yet to be elucidated.

The purpose of our study, therefore, was to evaluate the role of GRASP MR imaging in localizing the pituitary gland in patients with macroadenomas with 3 readers with vastly varying levels of expertise and to correlate such localization with intraoperative findings.

MATERIALS AND METHODS
Patients
An institutional review board–approved Health Insurance Portability and Accountability Act–compliant study was performed. We retrospectively identified patients with macroadenomas who underwent trans-sphenoidal surgery from November 2014 through November 2015. Of these, only those patients who had undergone preoperative dynamic MR imaging evaluation at our institution with GRASP were considered. Patients who had prior partial or subtotal resection of the macroadenoma were excluded from the study. Seventeen patients were included.

MR Imaging
All patients underwent MR imaging at 3T (Magnetom Skyra; Siemens, Erlangen, Germany) with a 20-channel head/neck coil. Imaging protocol included a coronal radial volumetric interpolated brain examination with a GRASP acquisition (TR/TE, 6.4/2.4 ms; 800 spokes at a 9.5° flip angle; 180×180 mm² in-plane FOV with a 256×256 matrix for a 0.7×0.7 mm² in-plane resolution at 391-Hz/pixel bandwidth; 32 sections, 0.8-mm-thick each, for a 180-second total acquisition time). This was followed by precontrast sagittal T1 (TR/TE, 440/2.66 ms; 160-mm² in-plane FOV; 320^2 matrix; 380-Hz/pixel bandwidth; 90° flip angle; 25 sections 3-mm-thick each), coronal T2 (TR/TE, 4000/97 ms; 15 sections, 2-mm-thick each; 140-mm² FOV; 320^2 matrix, at 260-Hz/pixel bandwidth; 150° flip angle), and axial FLAIR sequences (TR/TE/TI, 9000/90/2500 ms; 220-mm² FOV; 320^2 matrix; 290-Hz/pixel bandwidth; 150° flip angle; 15 sections, 5-mm-thick each). Gadopentetate dimeglumine (Magnevist; Bayer HealthCare Pharmaceuticals, Wayne, New) contrast material at 0.01 mmol per kilogram of body weight was administered at 4 mL/s on initiation of the GRASP acquisition.

Image Data Analysis and Processing
The acquired data from GRASP scans were exported and reconstructed off-line by using a C++ implementation of the GRASP algorithm, creating 9 dynamic image frames with a temporal resolution of 20 seconds each. Reconstructed images were sent to the PACS and were analyzed by using the software Olea Sphere, Version 2.3 (Olea Medical, La Ciotat, France). Permeability measurements were performed, including enhancement-time curves (ETCs) and peak enhancement.

To ascertain how robust the GRASP image interpretation was to readers' experience, 3 independent readers with vastly varying levels of neuroradiology experience evaluated the images: a medical student, a radiology resident (postgraduate year 4), and an attending neuroradiologist (with 15 years of neuroradiology experience). We evaluated the pituitary gland and macroadenoma by placing 2 ROIs, 1 within each of these 2 locations, and obtained permeability measurements (peak) and ETCs for each. Sagittal reconstructions confirmed the placement of the ROIs within their respective locations. We then compared the location of the gland in 3D between observers and correlated our measurements with the intraoperative location as per the surgeon's operative report.

Statistical Analysis
All statistics were performed in SPSS, Version 23.0 (IBM, Armonk, New York). The analysis was divided into 2 parts. First, the Fleiss κ test was performed on all 17 cases to determine the level of agreement among the 3 readers in rating the gland position in each plane (superior versus inferior, anterior versus posterior, right versus left) and the exact 3D position (eg, right anterosuperior, left posteroinferior, and so forth), irrespective of the operative findings. Subsequently, after we excluded cases in which operative findings of adenoma localization were ambiguous or indeterminate ($n = 4$), we repeated the same Fleiss κ calculation on the remaining 13 cases, comparing our readers' performance with definitive operative findings, both as a group and individually.

RESULTS
During our study period, 17 patients were included. Of these, 7 were women and 10 were men, with an age range of 22–69 years. The macroadenoma size ranged from 3.3 to 37.7 cm³, with a median of 7.8 cm³. Only 6 macroadenomas were homogeneous, 10 demonstrated necrosis, and 6 contained hemorrhage. Four of the operative reports did not contain complete localization data and were excluded from the calculation of observer agreement with intraoperative findings. Localization was determined in all 3 planes.

The interobserver agreement in our study was excellent, with a total characterization of $\kappa = 0.89$. The agreement in the transverse and coronal planes was slightly better than that in the sagittal plane: $\kappa = 0.85$, $\kappa = 0.86$, and $\kappa = 0.63$, respectively.

When we compared the readers' preoperative localizations with the operative reports, the overall characterization in all 3 planes was excellent ($\kappa = 0.95$). There was perfect agreement in the coronal and transverse planes, $\kappa = 1.0$, while agreement in the anteroposterior dimension was slightly less at $\kappa = 0.78$.

Evaluation of the ETCs derived from the pituitary gland and the macroadenoma showed greater peak enhancement in the normal gland (1014 versus 635.5, $P < .001$). Also, the ETC was noted to be steeper in the gland compared with the adenoma (Fig 1).

DISCUSSION
Our study demonstrates the role of preoperative, contrast-enhanced dynamic MR imaging to accurately and consistently differentiate the pituitary gland from the macroadenoma. Using GRASP reconstruction, we were able to confirm our localization with quantitative measures such as ETCs and peak enhancement values.

Dynamic contrast-enhanced MR imaging is the criterion standard for evaluating sellar-based lesions.[7-9] In contrast to cases of microadenomas in which identifying the tumor itself is the primary objective, cases of macroadenomas require evaluation of tumor extension into adjacent structures, including supra- and parasellar regions. For the surgeon, in addition to assessing such tumoral extension, localizing the pituitary gland becomes impor-
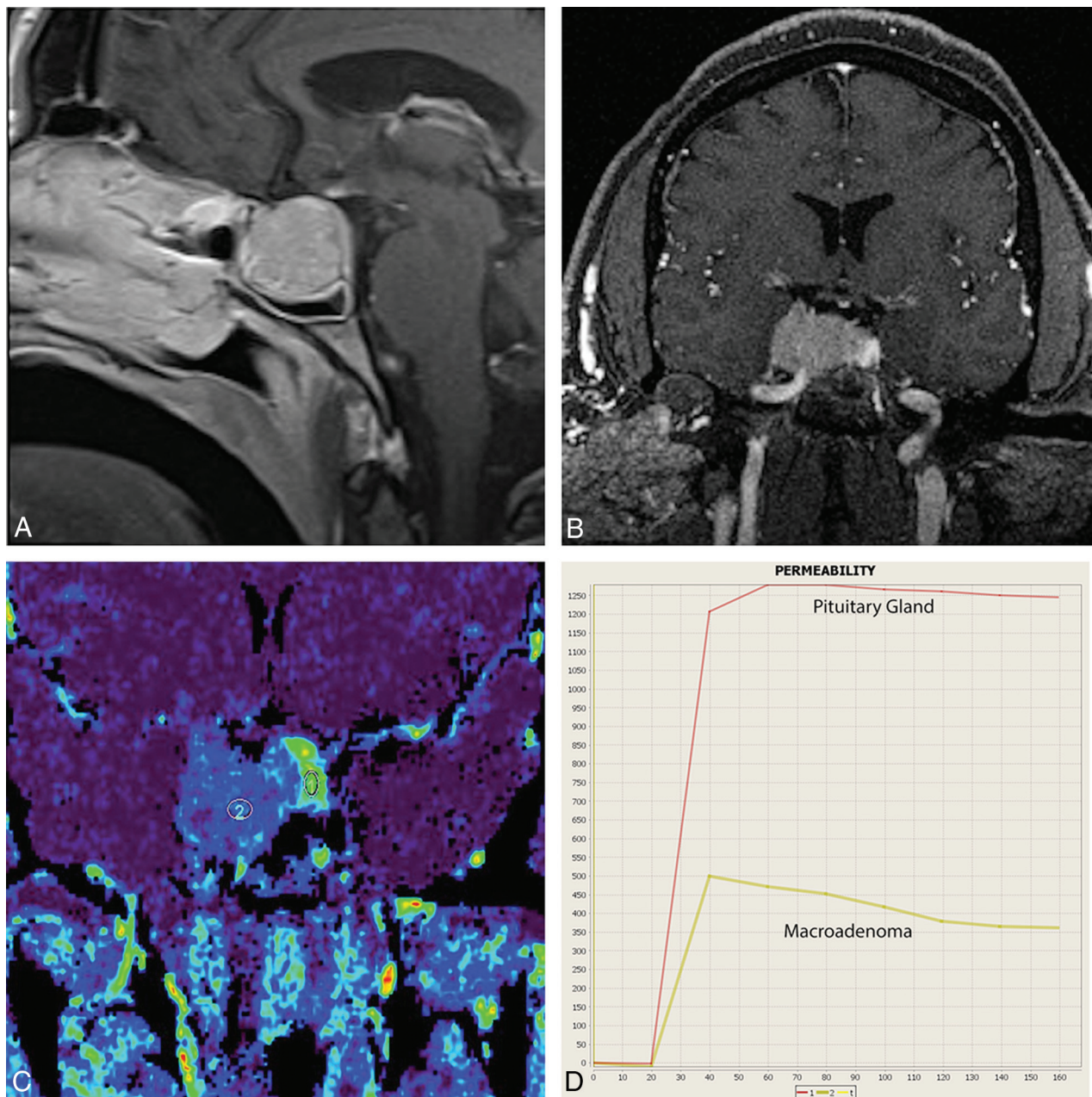
FIG 1. *A*, Contrast-enhanced sagittal T1WI demonstrates a macroadenoma. *B*, GRASP dynamic MR imaging through the sella demonstrates the macroadenoma extending into the right cavernous sinus. A focal area of increased enhancement is seen along the left lateral aspect of lesions. *C*, Postprocessed MR permeability peak scan demonstrates a focal area of increased contrast uptake (ROI 1) from the left lateral aspect of the sella compared with the macroadenoma (ROI 2). *D*, The enhancement-time curve confirms that the normal pituitary gland, localized along the left lateral aspect of the sella, enhances earlier and more robustly than the macroadenoma.

tant to minimize hormonal deficiency postoperatively. Such preoperative localization of the pituitary gland can be challenging.

The GRASP 3D gradient-echo MR imaging sequence for dynamic imaging provides the reader with markedly enhanced spatial and temporal resolution compared with conventional dynamic MR imaging sequences. This study aimed to take advantage of these improved features to preoperatively localize the pituitary gland distinct from macroadenomas and to confirm such localization with intraoperative findings.

Using permeability measures, we found minimal interobserver variability in identifying the gland within the macroadenoma in both the coronal and sagittal planes. The κ score in the

anteroposterior dimension was slightly lower at $\kappa = 0.63$, which we believe is due to our limitations in viewing the most appropriate section in the sagittal plane. Overall, these results highlight the reliability of this tool in identifying the pituitary gland. Furthermore, the range of training levels among the 3 readers emphasizes the ease of use of the software.

An additional benefit to this study was in its use of ETCs to validate the ROI placement. It is well-known that the pituitary gland is more avidly contrast-enhancing than the macroadenoma.[17-19] This feature is likely due to the differences in the vasculature of the normal and adenomatous pituitary tissue. Several previous studies have shown histologically that the normal
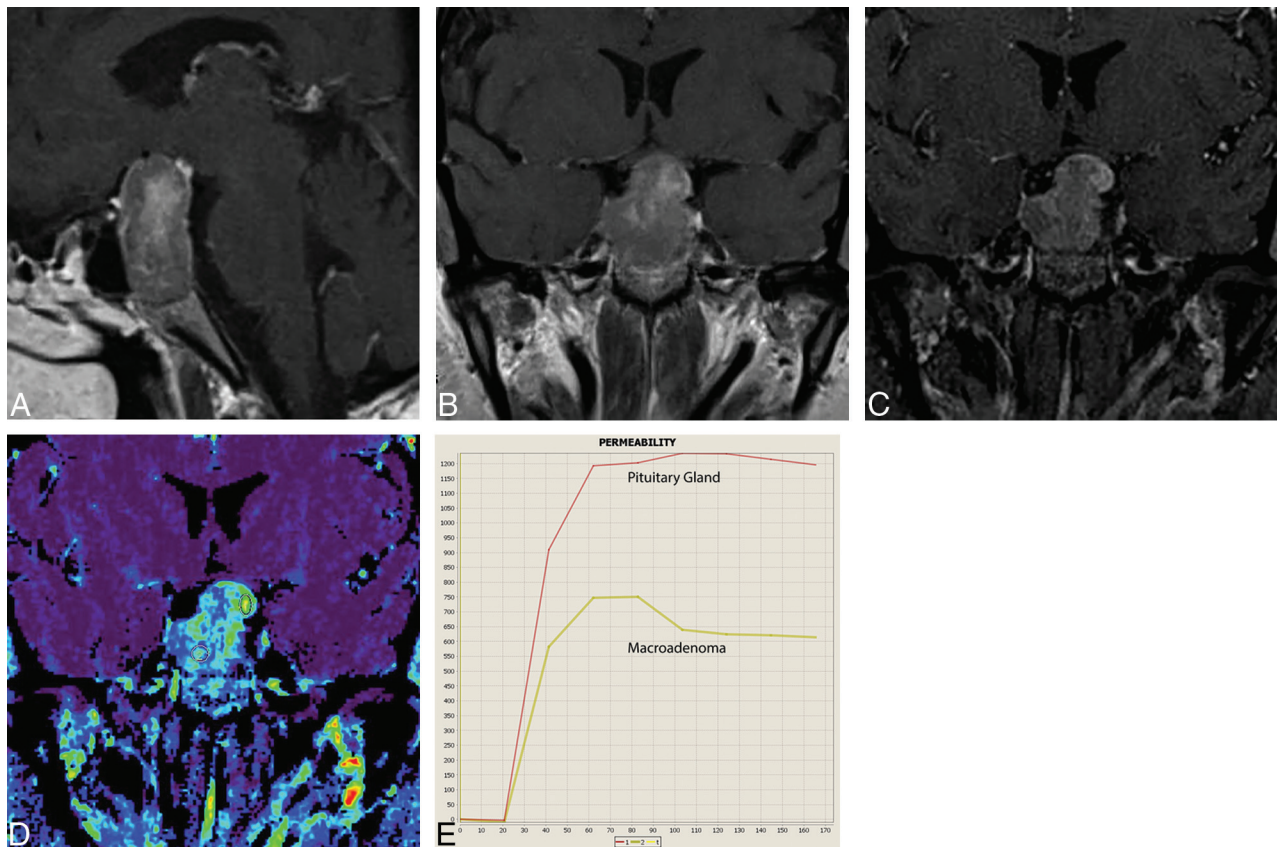
FIG 2. *A*, Contrast-enhanced sagittal T1WI through the sella demonstrates a heterogeneously enhancing lesion expanding the sella and extending into the suprasellar compartment, suggestive of a macroadenoma. *B*, Contrast-enhanced coronal T1WI demonstrates the macroadenoma. The heterogeneous enhancement within the lesion makes it difficult to localize the pituitary gland. *C*, GRASP dynamic study at 90 seconds (early dynamic phase) demonstrates more prominent enhancement along the left superolateral aspect of the lesion. *D*, Wash-in permeability study with ROIs placed within the central, heterogeneous portion of the lesion (ROI 2) and the more avidly enhancing region seen along its left superolateral aspect (ROI 1). *E*, Enhancement-time curves demonstrate a difference in rate and peak contrast uptake for each ROI. The ROI from the more avidly enhancing component seen along the left superolateral aspect of the lesion demonstrates a more pronounced peak enhancement than the more central, heterogeneously enhancing component. These curves validate that the pituitary gland is localized along the left superolateral aspect of this lesion, which was also confirmed at the operation.

pituitary gland is more highly vascularized than a pituitary adenoma.[20,21] Furthermore, more recent studies have used objective mathematic models to prove that the vascular supply to the normal pituitary gland is a more complex and well-organized microvascular network than that of a pituitary adenoma.[22,23] This feature subsequently leads to more robust blood flow to the normal pituitary gland and presumably more avid contrast enhancement. We were able to use this inherent difference between the 2 tissues to support our ROI placement because the ETC for the pituitary gland had a significantly greater peak enhancement and a relatively steeper slope than that of the macroadenoma. The use of ETCs can be particularly useful when confronted with heterogeneously enhancing macroadenomas, in which the normal gland is difficult to visualize with the naked eye (Fig 2).

After establishing reader agreement, we assessed our accuracy using intraoperative findings as a representation of the true gland location within the tumor. When we compared the readers' localizations with the intraoperative locations, 4 of the 17 cases were excluded, given the uncertainty in the operating room regarding the pituitary gland location. Analysis of the remaining 13 cases led to $\kappa = 0.95$ between readers and intraoperative findings. In fact, all 3 readers were perfect in identifying the pituitary gland in the

coronal and transverse planes with variability occurring only in the sagittal plane. These results validate the ability of readers with various degrees of experience to use the GRASP MR imaging sequence and ETCs to accurately identify the pituitary gland in patients with macroadenomas.

To further validate this largely qualitative method of gland localization, we compared the quantitative measurement of peak enhancement between the pituitary gland and a macroadenoma. As predicted, the pituitary gland had a statistically higher mean peak contrast value compared with the tumor (1014 versus 635.5).

To our knowledge, only 1 previous study using dynamic MR imaging has tried to localize the pituitary gland in patients with macroadenomas.[24] Using dynamic MR imaging and multidetector-row CT imaging, this group found that they were able to correctly identify the gland in 28 of 33 cases. However, the authors relied solely on subjective visualization of the preoperative scan. There was no quantitative measure confirmation. In addition, the authors did not mention the mean size of the macroadenomas in their patient population. This is an important consideration because normal pituitary gland localization can be difficult in larger macroadenomas; hence, submillimeter voxel thickness is of great

importance when acquiring the data. In the aforementioned study, 3-mm-thick sections were used for performing dynamic studies.

The implications of our results cover a range of areas, which include facilitating surgical planning, influencing better endocrine outcomes, and minimizing operative time, which can lead to an overall reduction of costs. Furthermore, this work has value for alternative therapeutic approaches, including pituitary tumor stereotactic radiosurgery.

Limitations to this study include its retrospective nature and the small sample size of 17 patients. Also, for particularly large macroadenomas of >4 cm in the craniocaudal dimension, evaluation of the gland was more challenging. Another limitation is the potential for the normal pituitary gland to shift intraoperatively, leading to a false preoperative localization. Last, the software used limited our ability to view the normal gland in the sagittal plane, making anteroposterior localization more variable. We plan to continue the work with a prospective study of a larger cohort along with exploring the role of this MR sequence in intraoperative navigation.

CONCLUSIONS

To our knowledge, clear identification of the pituitary gland in patients with macroadenoma has not been thoroughly studied, most likely due to the limitations in the resolution of current MR imaging sequences. Given that endocrine insufficiency is the most common complication of trans-sphenoidal surgery for macroadenomas, accurate localization of the gland preoperatively may provide surgeons with valuable information to preserve endocrine function. We have demonstrated the utility of dynamic GRASP MR imaging in successfully localizing the pituitary gland in patients with macroadenomas, and we supported our findings with quantitative permeability measurements.

REFERENCES

1. Ciric I, Ragin A, Baumgartner C, et al. **Complications of transsphenoidal surgery: results of a national survey, review of the literature, and personal experience.** *Neurosurgery* 1997;40:225–36; discussion 236–37 CrossRef Medline
2. Ciric I, Mikhael M, Stafford T, et al. **Transsphenoidal microsurgery of pituitary macroadenomas with long-term follow-up results.** *J Neurosurg* 1983;59:395–401 CrossRef Medline
3. Chabot JD, Chakraborty S, Imbarrato G, et al. **Evaluation of outcomes after endoscopic endonasal surgery for large and giant pituitary macroadenoma: a retrospective review of 39 consecutive patients.** *World Neurosurg* 2015;84:978–88 CrossRef Medline
4. Zhao B, Wei YK, Li GL, et al. **Extended transsphenoidal approach for pituitary adenomas invading the anterior cranial base, cavern-ous sinus, and clivus: a single-center experience with 126 consecutive cases.** *J Neurosurg* 2010;112:108–17 CrossRef Medline
5. Pinar E, Yuceer N, Imre A, et al. **Endoscopic endonasal transsphenoidal surgery for pituitary adenomas.** *J Craniofac Surg* 2015;26:201–05 CrossRef Medline
6. Juraschka K, Khan OH, Godoy BL, et al. **Endoscopic endonasal transsphenoidal approach to large and giant pituitary adenomas: institutional experience and predictors of extent of resection.** *J Neurosurg* 2014;121:75–83 CrossRef Medline
7. Hofstetter CP, Shin BJ, Mubita L, et al. **Endoscopic endonasal transsphenoidal surgery for functional pituitary adenomas.** *Neurosurg Focus* 2011;30:E10 CrossRef Medline
8. Ceylan S, Koc K, Anik I. **Endoscopic endonasal transsphenoidal approach for pituitary adenomas invading the cavernous sinus.** *J Neurosurg* 2010;112:99–107 CrossRef Medline
9. Fatemi N, Dusick JR, Mattozo C, et al. **Pituitary hormonal loss and recovery after transsphenoidal adenoma removal.** *Neurosurgery* 2008;63:709–18; discussion 718–19 CrossRef Medline
10. Lee HB, Kim ST, Kim HJ, et al. **Usefulness of the dynamic gadolinium-enhanced magnetic resonance imaging with simultaneous acquisition of coronal and sagittal planes for detection of pituitary microadenomas.** *Eur Radiol* 2012;22:514–18 CrossRef Medline
11. Chandarana H, Block TK, Rosenkrantz AB, et al. **Free-breathing radial 3D fat-suppressed T1-weighted gradient echo sequence: a viable alternative for contrast-enhanced liver imaging in patients unable to suspend respiration.** *Invest Radiol* 2011;46:648–53 CrossRef Medline
12. Chandarana H, Feng L, Block TK, et al. **Free-breathing contrast-enhanced multiphase MRI of the liver using a combination of compressed sensing, parallel imaging, and golden-angle radial sampling.** *Invest Radiol* 2013;48:10–16 CrossRef Medline
13. Winkelmann S, Schaeffter T, Koehler T, et al. **An optimal radial profile order based on the Golden Ratio for time-resolved MRI.** *IEEE Trans Med Imaging* 2007;26:68–76 CrossRef Medline
14. Feng L, Grimm R, Block KT, et al. **Golden-angle radial sparse parallel MRI: combination of compressed sensing, parallel imaging, and golden-angle radial sampling for fast and flexible dynamic volumetric MRI.** *Magn Reson Med* 2014;72:707–17 CrossRef Medline
15. Usman M, Atkinson D, Odille F, et al. **Motion corrected compressed sensing for free-breathing dynamic cardiac MRI.** *Magn Reson Med* 2013;70:504–16 CrossRef Medline
16. Rossi Espagnet MC, Bangiyev L. **High-resolution DCE-MRI of the pituitary gland using radial k-space acquisition with compressed sensing reconstruction.** *AJNR Am J Neuroradiol* 2015;36:1444–49 CrossRef Medline
17. Miki Y, Matsuo M, Nishizawa S, et al. **Pituitary adenomas and normal pituitary tissue: enhancement patterns on gadopentetate-enhanced MR imaging.** *Radiology* 1990;177:35–38 CrossRef Medline
18. Yuh WT, Fisher DJ, Nguyen HD, et al. **Sequential MR enhancement pattern in normal pituitary gland and in pituitary adenoma.** *AJNR Am J Neuroradiol* 1994;15:101–08 Medline
19. Lundin P, Bergström K. **Gd-DTPA-enhanced MR imaging of pituitary macroadenomas.** *Acta Radiol* 1992;33:323–32 Medline
20. Schechter J. **Ultrastructural changes in the capillary bed of human pituitary tumors.** *Am J Pathol* 1972;67:109–26 Medline
21. Gorczyca W, Hardy J. **Microadenomas of the human pituitary and their vascularization.** *Neurosurgery* 1988;22:1–6 Medline
22. Di Ieva A, Weckman A, Di Michele J, et al. **Microvascular morphometrics of the hypophysis and pituitary tumors: from bench to operating theatre.** *Microvasc Res* 2013;89:7–14 CrossRef Medline
23. Di Ieva A, Grizzi F, Ceva-Grimaldi G, et al. **Fractal dimension as a quantitator of the microvasculature of normal and adenomatous pituitary tissue.** *J Anat* 2007;211:673–80 CrossRef Medline
24. Miki Y, Kanagaki M, Takahashi JA, et al. **Evaluation of pituitary macroadenomas with multidetector-row CT (MDCT): comparison with MR imaging.** *Neuroradiology* 2007;49:327–33 CrossRef Medline